A New Colloid Model for Dissipative-Particle-Dynamics Simulations

Jiajia Zhou and Friederike Schmid

Abstract We propose a new model to simulate spherical colloids. This is a mesoscopic method based on the dissipative particle dynamics. The colloid is represented by a large spherical bead, and its surface interacts with the solvent beads through a pair of dissipative and stochastic forces. This new model extends the tunable-slip boundary condition [Eur. Phys. J. E **26**, 115 (2008)] from planar surfaces to curved geometry, thus allows one to study colloids with slippery surfaces. Simulation results show good agreement with the prediction of hydrodynamic theories, indicating the hydrodynamic interactions are properly accounted in our new model.

1 Introduction

Colloidal dispersions have many scientific interests and practical applications in various fields such as soft matter physics, physical chemistry, cell biology, medicine development, and micro- or nanofluidic devices [1, 2]. In an aqueous solution, colloidal particles in general have a typical size one order of magnitude larger than the small solvent molecules. This separation of length scales presents a significant challenge in simulating the dynamics of colloidal particles: On one hand, explicit consideration of the solvent with molecular details imposes a huge burden on the computational time, while most interesting phenomena may not concern solvents. On the other hand, the solvents cannot to totally ignored because they mediate the hydrodynamic interactions between larger colloidal particles. This dilemma is somewhat alleviated by resorting to coarse-grained simulations, in which the solvent degree of freedom are greatly reduced while hydrodynamic interactions are still preserved by enforcing the conservation of several physical quantities, such as the particle number and the momentum. Coarse-graining approaches allow one to study larger sys-

Jiajia Zhou · Friederike Schmid
Institut für Physik, Johannes Gutenberg-Universität Mainz, Staudingerweg 9, D55099 Mainz, Germany, e-mail: zhou@uni-mainz.de, friederike.schmid@uni-mainz.de

tem and reach longer time scale. Notable examples are dissipative particle dynamics (DPD) [3, 4, 5, 6], Lattice Boltzmann (LB) [7, 8, 9], Multi-Particle Collision Dynamics (MPCD) [10, 11], and Direct Numerical Simulation (DNS) [12, 13, 14, 15].

Once one settles on a mesoscopic model for the solvent, the next task is to build a colloid model which couples to the solvent. From a simulation point of view, one would like a colloid model which is conceptually simple and easy to implement, but also represents the correct physics. There are several approaches:

- *Discretization of Large Colloid*
  Based on the initial DPD formulation, Hoogerbrugge and Koelman [3, 4] constructed the colloid using the same solvent beads. The relative motion of these small beads is "frozen" so the integrity of the large colloid is kept. Similar approach has been implemented to study many interacting colloids in microfluidic devices [16]. This "frozen particle" model is relatively simple because the beads in the colloid interact with the solvent through the same DPD interactions, and no extra parameters are required. A conceptually similar approach has been proposed in Lattice Boltzmann simulations: the so-called raspberry model presents the colloid as a collection of the surface beads. The surface beads couple to the LB fluids by a viscous force which depends on the relative velocity of the beads to the local fluids [17]. The positions of the surface beads are maintained either by a spring force [18, 19] or by fixing the bead position with respect to the colloid center [20, 21]. One drawback of the raspberry model is that the interacting beads occurs only on the surface and the fluid is allowed to penetrate inside the hollow sphere. It was later demonstrated to cause a discrepancy between the translational and rotational diffusion [22]. This can be remedied by adding the internal coupling points [23, 24]. Raspberry model was also implemented in DPD simulations [25, 26, 27, 28], where we used a repulsive interaction to prevent solvent penetration.

- *Using Single Large Bead*
  Español proposed the fluid particle model (FPM) [29] which treats the colloid as one single object instead of combination of small particles. To model the large colloids, two additional non-central shear components are incorporated into the dissipative forces. Similar model has been proposed by Pan *et. al.* [30].

- *Boundary Condition*
  Colloids can also be implemented as the boundary condition, which is common in LB and MPCD simulations. Ladd had constructed the colloid as an extended hollow sphere where bounce-back collision rules are applied on the colloid surfaces [31, 32, 33]. In MPCD, the coupling between the immersed colloids and the solvent can be implemented by either bounce-back rules or thermal wall boundary condition [34, 35, 36, 37].

Most of the colloid models are designed to realize the no-slip boundary condition on colloid surfaces. But for certain colloids with hydrophobic surfaces, slippage can occur. We have proposed tunable-slip boundary condition for flat surfaces in DPD

[38, 39, 40, 41, 42, 43, 44, 45], which allows one to set the local slip length. In this work, we present a colloid model based on the tunable-slip boundary condition. The remainder of this article is organized as follows: In section 2, we introduce the colloid model and describe relevant parameters in simulation. We present the simulation results of diffusion constant in section 3. Finally, we conclude in section 4 with a brief summary.

2 Marble Model

To facilitate the discussion, we first present a short introduction to the traditional DPD. We then describe our new colloid model based on the same notation.

Dissipative Particle Dynamics is an well-established simulation method for mesoscale fluid. For two solvent beads i and j, their relative displacement is denoted by $\mathbf{r}_{ij} = \mathbf{r}_i - \mathbf{r}_j$ and their relative velocity $\mathbf{v}_{ij} = \mathbf{v}_i - \mathbf{v}_j$ (see Fig. 1). The force exerted by bead j on i is given by a pair of dissipative and random forces,

$$\mathbf{F}_{ij}^{\mathrm{DPD}} = \mathbf{F}_{ij}^{\mathrm{D}} + \mathbf{F}_{ij}^{\mathrm{R}}. \tag{1}$$

The dissipative force $\mathbf{F}_{ij}^{\mathrm{D}}$ is proportional to the relative velocity between two beads,

$$\mathbf{F}_{ij}^{\mathrm{D}} = -\gamma^{\mathrm{DPD}}\, \omega^{\mathrm{D}}(r_{ij})(\mathbf{v}_{ij} \cdot \hat{\mathbf{r}}_{ij})\hat{\mathbf{r}}_{ij}, \tag{2}$$

with a friction coefficient γ^{DPD} and a weight function ω^{D},

$$\omega^{\mathrm{D}}(r) = \begin{cases} \left(1 - \dfrac{r}{r_{\mathrm{c}}}\right)^2 & \text{if } r \le r_{\mathrm{c}}^{\mathrm{DPD}}, \\ 0 & \text{if } r > r_{\mathrm{c}}^{\mathrm{DPD}}. \end{cases} \tag{3}$$

The cutoff radius $r_{\mathrm{c}}^{\mathrm{DPD}}$ characterizes the finite range of the interaction.

The random component $\mathbf{F}_{ij}^{\mathrm{R}}$ has the form

$$\mathbf{F}_{ij}^{\mathrm{R}} = \sqrt{2k_B T \gamma^{\mathrm{DPD}}\, \omega^{\mathrm{D}}(r_{ij})}\, \xi\, \hat{\mathbf{r}}_{ij}, \tag{4}$$

where ξ is a random number with zero mean $\langle \xi(t) \rangle = 0$ and variance $\langle \xi(t)\xi(t') \rangle = \delta(t-t')$. The dissipative and random forces are related by the fluctuation-dissipation theorem, so to maintain the proper temperature in the simulation. The forces between two beads are the same in magnitude but opposite in direction, $\mathbf{F}_{ij}^{\mathrm{DPD}} = -\mathbf{F}_{ji}^{\mathrm{DPD}}$, hence the momentum is conserved. The conservation of momentum is essential for DPD to obtain the correct long-time hydrodynamic behavior.

In the following, physical quantities will be reported in a unit system of σ (length), m (mass), ε (energy), and a derived time unit $\tau = \sigma\sqrt{m/\varepsilon}$. We use a solvent density $\rho = 3.0\,\sigma^{-3}$. The friction coefficient for the solvent is $\gamma^{\mathrm{DPD}} =$

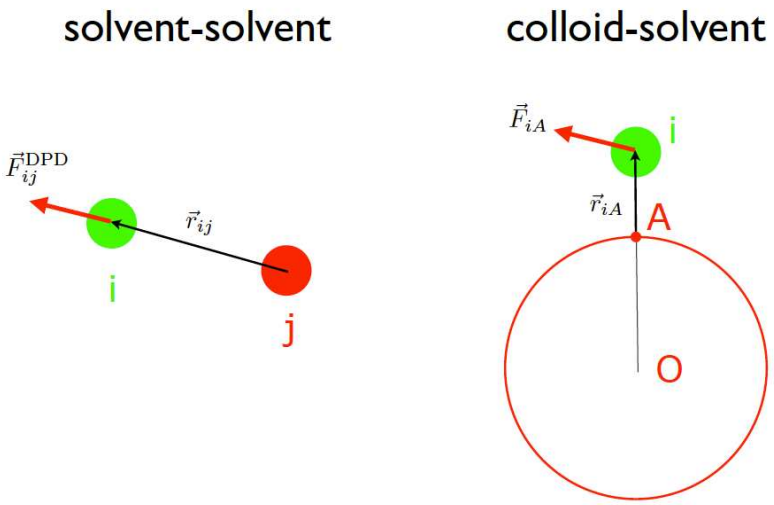

Fig. 1 Sketches to demonstrate the solvent-solvent interaction (left) and colloid-solvent interaction (right).

$5.0\,m/\tau$ and the cutoff $r_{\mathrm{c}}^{\mathrm{DPD}} = 1.0\,\sigma$. The shear viscosity is measured as $\eta_s = 1.23 \pm 0.01\,m/(\sigma\tau)$.

The colloidal particle is represented by a large spherical bead of radius $R = 3.0\,\sigma$. To prevent the solvent penetration, a modified Lennard-Jones interaction is applied between the colloid and the solvent,

$$V(r) = \begin{cases} 4\varepsilon \left[\left(\dfrac{\sigma}{r - r_0} \right)^{12} - \left(\dfrac{\sigma}{r - r_0} \right)^{6} + \dfrac{1}{4} \right] & \text{if } r - r_0 \le r_{\mathrm{c}}^{\mathrm{LJ}}, \\ 0 & \text{if } r - r_0 > r_{\mathrm{c}}^{\mathrm{LJ}}, \end{cases} \tag{5}$$

where $r_0 = 2.0\,\sigma$ and $r_{\mathrm{c}}^{\mathrm{LJ}} = 1.0\,\sigma$.

We image that at each time step, the solvent bead interacts with the colloid through the surface point A, which is located at the intersection of the colloid surface and the line connecting the solvent bead and the colloid center (see Fig. 1). The velocity of the surface point is given by

$$\mathbf{v}_A = \mathbf{v}_O + \omega \times \mathbf{r}_{OA}, \tag{6}$$

where $\mathbf{v}_O$ is center-of-mass speed and ω is the angular velocity of the colloid.

Similar to the interaction between two solvent beads, the forces between the solvent bead i and the surface point A consist of a dissipative and random components.

$$\mathbf{F}_{iA} = \mathbf{F}_{iA}^{\mathrm{D}} + \mathbf{F}_{iA}^{\mathrm{R}}. \tag{7}$$

There are at least three choices in setting the interaction between the colloid and the solvent:

1. *Traditional DPD Interaction.* One can use the traditional DPD interactions, just to think there is a solvent bead sitting at the surface point A,

$$\mathbf{F}_{iA}^{\mathrm{D}} = -\gamma\omega^{\mathrm{D}}(r_{iA})[(\mathbf{v}_i - \mathbf{v}_A)\cdot\hat{\mathbf{r}}_{iA}]\,\hat{\mathbf{r}}_{iA} \tag{8}$$

$$\mathbf{F}_{iA}^{\mathrm{R}} = \sqrt{2k_BT\gamma\omega^{\mathrm{D}}(r_{iA})}\,\xi\hat{\mathbf{r}}_{iA} \tag{9}$$

   where γ characterizes the coupling strength and ω^{D} is the same as in Eq. (3).

2. *Transverse Interaction.* The second possibility is to use the transverse interactions, which project the traditional DPD interactions on the plane perpendicular to the vector $\mathbf{r}_{iA}$ [46],

$$\mathbf{F}_{iA}^{\mathrm{D}} = -\gamma\omega^{\mathrm{D}}(r_{iA})\mathscr{P}(\mathbf{v}_i - \mathbf{v}_A) \tag{10}$$

$$\mathbf{F}_{iA}^{\mathrm{R}} = \sqrt{2k_BT\gamma\omega^{\mathrm{D}}(r_{iA})}\mathscr{P}(\hat{\xi}) \tag{11}$$

   where $\mathscr{P} = \mathscr{I} - \hat{\mathbf{r}}_{iA}\otimes\hat{\mathbf{r}}_{iA}$ is the projection operator and $\hat{\xi}$ is a vector whose three component are random numbers.

3. *Tunable-slip Interaction.* In the tunable-slip approach, the dissipative component is directly proportional to the relative velocity $\mathbf{v}_i - \mathbf{v}_A$. We implement this approach in our simulations, to be consistent with our previous works on the flat surfaces.

$$\mathbf{F}_{iA}^{\mathrm{D}} = -\gamma\omega^{\mathrm{D}}(r_{iA})(\mathbf{v}_i - \mathbf{v}_A) \tag{12}$$

$$\mathbf{F}_{iA}^{\mathrm{R}} = \sqrt{2k_BT\gamma\omega^{\mathrm{D}}(r_{iA})}\,\hat{\xi} \tag{13}$$

The total force exerted on the colloid is a summation over all solvent beads which are less than 1.0σ away from the colloid surface,

$$\mathbf{F}^{\mathrm{C}} = \sum_i \mathbf{F}_{Ai} + \mathbf{F}^{\mathrm{LJ}}. \tag{14}$$

Similarly, the total torque exerted on the colloid is

$$\mathbf{T}^{\mathrm{C}} = \sum_{i=1} \mathbf{F}_{Ai}\times(\mathbf{r}_A - \mathbf{r}_O), \tag{15}$$

The total force and torque are then used to update the position and velocity of the colloid in one time step using the Velocity-Verlet algorithm. All simulations were carried out using the open source package ESPResSo [47].

3 Results and Discussions

To test our new colloid model, we simulate a single colloid in a cubic box of size L. We measure the diffusion constant of the colloid using three different methods and compare the result to the hydrodynamic theory.

The first method computes the diffusion constant through the autocorrelation functions. We obtain two correlation functions from the simulations: the translational and rotational velocity autocorrelation functions

$$C_v(t) = \frac{\langle \mathbf{v}(0) \cdot \mathbf{v}(t) \rangle}{\langle \mathbf{v}^2 \rangle}, \tag{16}$$

$$C_\omega(t) = \frac{\langle \omega(0) \cdot \omega(t) \rangle}{\langle \omega^2 \rangle}, \tag{17}$$

where $\mathbf{v}(t)$ and $\omega(t)$ are the translational velocity and rotational velocity of the colloid at time t, respectively. Using the Green-Kubo relation, we obtain the diffusion constant of the colloid by integrating the translational velocity autocorrelation function

$$D = \frac{1}{3} \int_0^\infty \mathrm{d}t \, \langle \mathbf{v}(0) \cdot \mathbf{v}(t) \rangle. \tag{18}$$

Figure 2 shows the simulation results for $\gamma = 5.0\, m/\tau$ in log-log plots. The autocorrelation functions show different behavior at short and long time scales. At short times, both autocorrelation functions decay exponentially. At long times, hydrodynamic interactions lead to a slow relaxation of algebraic decay, which is called long-time tail [48]. Mode-coupling theory predicts the coefficient of algebraic decay at long times to be $-\frac{3}{2}$ for the translational velocity and $-\frac{5}{2}$ for the rotational velocity [49]. These predictions are plotted as green lines in Fig. 2. The simulation results are consistent with the theoretical prediction for $t > 10\,\tau$, but both autocorrelation functions exhibit large fluctuation. This is due to the poor statistics for long-time values of the correlation function. One can improve the results by running very long simulations.

The second method to measure the diffusion constant is by calculation of the mean squared displacement. From Einstein relation

$$\lim_{t\to\infty} \langle (\mathbf{r}(t) - \mathbf{r}(0))^2 \rangle = 6Dt, \tag{19}$$

where $\mathbf{r}$ is the position of the colloid center. Figure 3 shows a typical mean squared displacement as a function of the time. At short times, the colloid exhibits a ballistic motion where the mean squared displacement increases as t^2. At later times, the ballistic motion is replaced by a diffusive motion where the mean squared displacement is proportional to t. A linear fit of the mean squared displacement at $t > 25\,\tau$ gives the diffusion constant.

The diffusion constant can also be obtained by a simulation experiment. We apply a constant force to the colloid. To prevent accelerating the whole system, we also apply a small force to each fluid bead, and the total force on the fluid is opposite

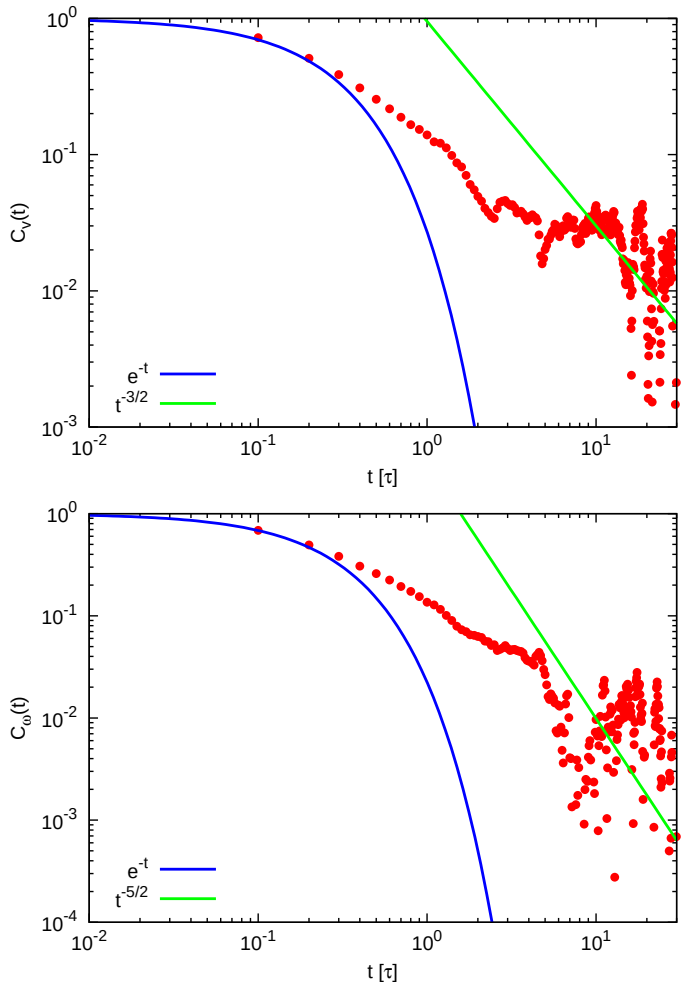

Fig. 2 Translational (top) and rotational (bottom) velocity autocorrelation functions in log-log plots. The simulation is performed for the following parameters: colloid radius $R = 3.0\sigma$, temperature $k_BT = 1.0\,\varepsilon$, and colloid-solvent parameter $\gamma = 5.0\,m/\tau$.

to the force on the colloid, and with the same magnitude. At late times, the colloid reaches a constant velocity $\mathbf{v}_f$ with respect to the fluid. In this stationary state, the external driving force is balanced by the viscous friction

$$\mathbf{F}_{\text{ext}} = -\gamma_C \mathbf{v}_f, \tag{20}$$

where γ is the friction coefficient. The fluctuation-dissipation theorem relates the friction coefficient to the diffusion constant by

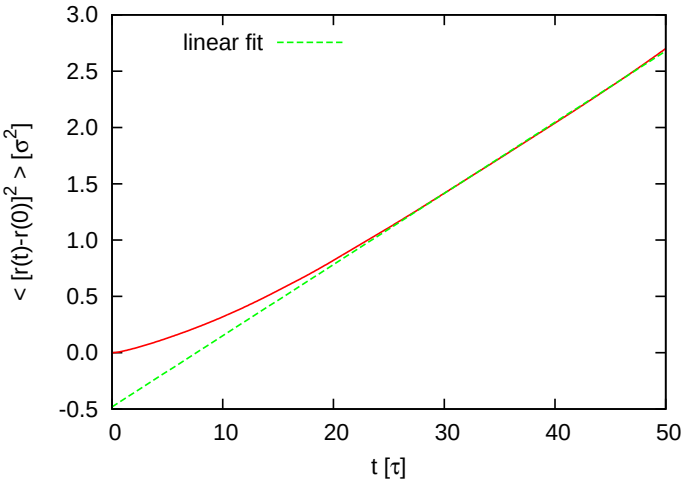

Fig. 3 The mean squared displacement of a spherical colloid with radius $R = 3.0\,\sigma$ in a cubic simulation box of sizes $L = 20\,\sigma$. The line shows a linear fit to data $t > 25\tau$.

$$D = \frac{k_B T}{\gamma_C}. \tag{21}$$

Figure 4 collects all simulation results obtained by three different methods [velocity autocorrelation function (vacf), mean squared displacement (msd), and force measurement (force)]. The diffusion constant is measured at different values of colloid-solvent friction coefficient γ. Error bars are calculated by three independent runs with different initial configurations. The force measurement shows relatively small error bars in comparison to the other two approaches.

Upon increasing γ, the surface property changes from slippery to no-slip, and the diffusion constant decreases accordingly. No-slip boundary condition can be realized by using a friction coefficient $\gamma > 5m/\tau$. By adjusting the γ value, one can set the surface boundary of the colloidal particle from no-slip to full-slip. This freedom provides possibilities to investigate the effect of hydrodynamic slip on the dynamics of colloidal particles [50, 51].

We use periodic boundary condition in the simulations. For small simulation box, the colloid can interact with its periodic images, resulting a box-size dependent diffusion constant. In general, the diffusion constant increases with increasing box size. Hasimoto presented an analytic expression for the diffusion constant in terms of a series expansion of $1/L$, the reciprocal of the box size [52],

$$D = \frac{k_B T}{6\pi\eta_s}\left(\frac{1}{R} - \frac{2.837}{L} + \frac{4.19R^2}{L^3} + \cdots\right). \tag{22}$$

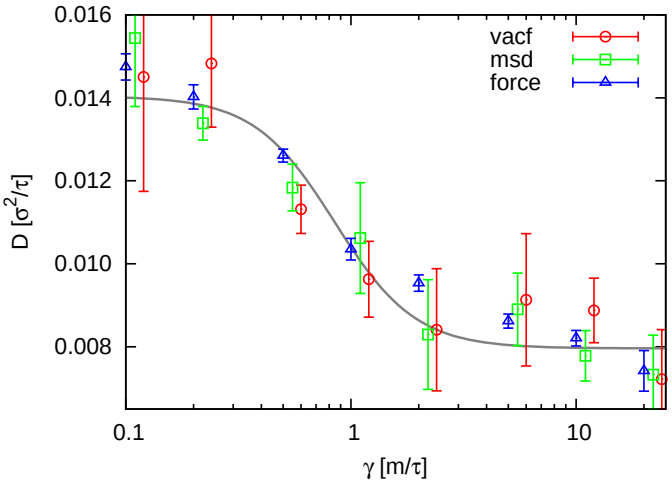

Fig. 4 The diffusion constant D for a spherical colloid of radius $R = 3.0\,\sigma$ as a function of the surface-solvent friction coefficient γ. The simulation box has a size of $L = 20\,\sigma$. The solid curve is a guide to the eyes. The data from autocorrelation function and mean squared displacement are shifted slightly in x-axis for a better view.

In Fig. 5, we plot the diffusion constant as a function of $1/L$, based on the force measurement. The simulation results show relatively well agreement to the Hasimoto formula, which is shown as the solid curve in Fig. 5.

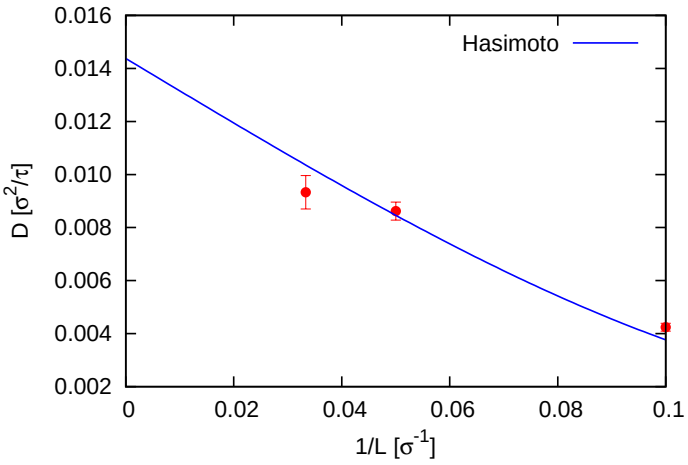

Fig. 5 The diffusion constant D for a spherical colloid of radius $R = 3.0\,\sigma$ as a function of $1/L$, the reciprocal of the box size. The curve is the prediction from Eq. (22).

4 Summary

We have developed a mesoscopic colloid model based on the dissipative particle dynamics. The colloid is represented by a large spherical bead, and its surface interacts with solvent beads through a pair of dissipative and random forces. We test this new colloid model by measuring the diffusion constant of a single colloid in a cubic box. The simulation results show good agreement with the predictions from hydrodynamic theories. Our model can be viewed as an extension of the tunable-slip boundary condition [38] to curved geometries, and allows one to investigate the dynamics of colloidal particles with slippery surfaces.

Acknowledgements

We thank the HLRS Stuttgart for a generous grant of computer time on HERMIT. This work is funded by the Deutsche Forschungsgemeinschaft (DFG) through SFB TR6 (subproject B9) and SFB 1066 (subproject Q1).

References

1. W.B. Russel, D.A. Saville, W. Schowalter, *Colloidal Dispersions* (Cambridge University Press, Cambridge, 1989)
2. J. Dhont, *An Introduction to Dynamics of Colloids* (Elsevier, Amsterdam, 1996)
3. P.J. Hoogerbrugge, J.M.V.A. Koelman, Europhys. Lett. **19**, 155 (1992)
4. J.M.V.A. Koelman, P.J. Hoogerbrugge, Europhys. Lett. **21**, 363 (1993)
5. P. Español, P.B. Warren, Europhys. Lett. **30**, 191 (1995)
6. R.D. Groot, P.B. Warren, J. Chem. Phys. **107**, 4423 (1997)
7. S. Succi, *The Lattice Boltzmann Equation* (Clarendon Press, Oxford, 2001)
8. D. Raabe, Modelling Simul. Mater. Sci. Eng. **12**, R13 (2004)
9. B. Dünweg, A.J.C. Ladd, Adv. Polym. Sci. **221**, 89 (2009)
10. A. Malevanets, R. Kapral, J. Chem. Phys. **110**, 8605 (1999)
11. G. Gompper, T. Ihle, D.M. Kroll, R.G. Winkler, Adv. Polym. Sci. **221**, 1 (2009)
12. H. Tanaka, T. Araki, Phys. Rev. Lett. **85**, 1338 (2000)
13. Y. Nakayama, R. Yamamoto, Phys. Rev. E **71**, 036707 (2005)
14. K. Kim, Y. Nakayama, R. Yamamoto, Phys. Rev. Lett. **96**, 208302 (2006)
15. Y. Nakayama, K. Kim, R. Yamamoto, Eur. Phys. J. E **26**, 361 (2008)
16. T. Steiner, C. Cupelli, R. Zengerle, M. Santer, Microfluid. Nanofluid. **7**, 307 (2009)
17. P. Ahlrichs, B. Dünweg, J. Chem. Phys. **111**, 8225 (1999)
18. V. Lobaskin, B. Dünweg, New Journal of Physics **6**, 54 (2004)
19. V. Lobaskin, B. Dünweg, M. Medebach, T. Palberg, C. Holm, Phys. Rev. Lett. **98**, 176105 (2007)
20. A. Chatterji, J. Horbach, J. Chem. Phys. **122**, 184903 (2005)
21. A. Chatterji, J. Horbach, J. Chem. Phys. **126**, 064907 (2007)
22. S.T.T. Ollila, C.J. Smith, T. Ala-Nissila, C. Denniston, Multiscale Model. Simul. **11**, 213 (2013)
23. L.P. Fischer, T. Peter, C. Holm, J. de Graaf, arXiv:1503.02671 [cond-mat.soft] (2015)
24. J. de Graaf, T. Peter, L.P. Fischer, C. Holm, arXiv:1503.02681 [cond-mat.soft] (2015)

25. J. Zhou, F. Schmid, J. Phys.: Condens. Matter **24**, 464112 (2012)
26. J. Zhou, F. Schmid, Eur. Phys. J. E **36**, 33 (2013)
27. J. Zhou, R. Schmitz, B. Dünweg, F. Schmid, J. Chem. Phys. **139**, 024901 (2013)
28. J. Zhou, F. Schmid, Eur. Phys. J. Special Topics **222**, 2911 (2013)
29. P. Español, Phys. Rev. E **57**, 2930 (1998)
30. W. Pan, I.V. Pivkin, G.E. Karniadakis, Europhys. Lett. **84**(1), 10012 (2008)
31. A. Ladd, Phys. Rev. Lett. **70**, 1339 (1993)
32. A. Ladd, J. Fluid Mech. **271**, 285 (1994)
33. A. Ladd, J. Fluid Mech. **271**, 311 (1994)
34. S.H. Lee, R. Kapral, J. Chem. Phys. **121**, 11163 (2004)
35. J.T. Padding, A. Wysocki, H. Löwen, A.A. Louis, J. Phys.: Condens. Matter **17**, S3393 (2005)
36. J.T. Padding, A.A. Louis, Phys. Rev. E **74**(3), 031402 (2006)
37. J.K. Whitmer, E. Luijten, J. Phys.: Condens. Matter **22**, 104106 (2010)
38. J. Smiatek, M. Allen, F. Schmid, Eur. Phys. J. E **26**, 115 (2008)
39. J. Smiatek, M. Sega, C. Holm, U.D. Schiller, F. Schmid, J. Chem. Phys. **130**, 244702 (2009)
40. J. Smiatek, F. Schmid, J. Phys. Chem. B **114**, 6266 (2010)
41. J. Smiatek, F. Schmid, Comput. Phys. Commun. **182**, 1941 (2011)
42. J. Zhou, A.V. Belyaev, F. Schmid, O.I. Vinogradova, J. Chem. Phys. **136**, 194706 (2012)
43. E.S. Asmolov, J. Zhou, F. Schmid, O.I. Vinogradova, Phys. Rev. E **88**, 023004 (2013)
44. J. Zhou, E.S. Asmolov, F. Schmid, O.I. Vinogradova, J. Chem. Phys. **139**, 174708 (2013)
45. T.V. Nizkaya, E.S. Asmolov, J. Zhou, F. Schmid, O.I. Vinogradova, Phys. Rev. E **91**, 033020 (2015)
46. C. Junghans, M. Praprotnik, K. Kremer, Soft Matter **4**, 156 (2008)
47. H. Limbach, A. Arnold, B. Mann, C. Holm, Comp. Phys. Comm. **174**, 704 (2006)
48. B.J. Alder, T.E. Wainwright, Phys. Rev. A **1**, 18 (1970)
49. J.P. Hansen, I.R. McDonald, *Theory of Simple Liquids*, 3rd edn. (Academic Press, London, 2006)
50. J.W. Swan, A.S. Khair, J. Fluid Mech. **606**, 115 (2008)
51. A.S. Khair, T.M. Squires, Phys. Fluids **21**, 042001 (2009)
52. H. Hasimoto, J. Fluid Mech. **5**, 317 (1959)